Steel and Composite Structures, *Vol. 23, No. 5 (2017) 543-555*
DOI: https://doi.org/10.12989/scs.2017.23.5.543

Mechanical properties of SFRHSC with metakaolin and ground pumice: Experimental and predictive study

Mustafa Sarıdemir*, Metin Hakan Severcan and Serhat Çelikten

Department of Civil Engineering, Ömer Halisdemir University, 51240 Niğde, Turkey

(*Received February 17, 2016, Revised January 12, 2017, Accepted January 24, 2017*)

Abstract. The mechanical properties of steel fiber reinforced high strength concrete (SFRHSC) made with binary and ternary blends of metakaolin (MK) and ground pumice (GP) are investigated in this study. The investigated properties are ultrasonic pulse velocity (U_{pv}), compressive strength (f_c), flexural strength (f_f) and splitting tensile strength (f_{st}) of SFRHSC. A total of 16 steel fiber reinforced concrete mixtures were produced by a total binder content of 500 kg/m^3 for determining the effects of MK and GP on the mechanical properties. The design f_c was acquired from 70 to 100 MPa by using a low water-binder ratio of 0.2. The test results exhibit that high strength concrete can be obtained by replacing the cement with MK and GP. Besides, correlations between these results are executed for comprehending the relationship between mechanical properties of SFRHSC and the strong correlations are observed between these properties. Moreover, two models in the gene expression programming (GEP) for predicting the f_c of SFRHSC made with binary and ternary blends of MK and GP have been developed. The results obtained from these models are compared with the experimental results. These comparisons proved that the results of equations obtained from these models seem to agree with the experimental results.

Keywords: steel fiber; metakaolin; ground pumice; strength properties; high strength concrete

1. Introduction

Recent developments in concrete technology reveal that the evaluation of mineral additives like metakaolin (MK), rice husk ash and silica fume (SF) is necessary for manufacturing high strength concrete (Parande *et al*. 2008, Bauchkar and Chore 2014). These materials, when employed as mineral additives instead of cement to manufacture high strength concrete, can develop the strength, impermeability and durability properties together with service life of concrete (Poon *et al*. 2006, Giaccio *et al*. 2007, Sarıdemir 2009). These additives provide extra performance to concrete through exposure to chemical reaction with cement hydration products to create extra calcium-silicate-hydrate (C-S-H) gel, which is the component of cement paste principally accountable for concrete strength (Neville 1996, Güneyisi *et al*. 2014). These additives can also reduce material costs due to low use of cement in the concrete production, and provide environmental advantages connected to the dispose of waste materials (Bui *et al*. 2005). Moreover, these additives decrease the porousness of concrete specifically at the interfaces between aggregate and cement paste that are the weakest areas of these materials. The improvements provided by the mineral supplements can change the failure mechanism of concrete (Giaccio *et al*. 2007).

SFRHSC is a concrete matrix composed with additions of fibers and mineral admixtures that enhance its mechanical properties. For manufacturing high performance concrete, many different types of fibers can be utilized like steel, glass, carbon and organic polymers (Ruano *et al*. 2014). Especially, many experimental studies have shown the advantages of using concrete containing steel fiber in construction applications, which comprise overlays, tunnel structures, precast concrete products, hydraulic structures, shotcrete applications, and special structures (Luccioni *et al*. 2012, Perumal 2014). The main benefit of steel fiber is the growth of tensile strain capacity of concrete using in these application areas (Kayali *et al*. 2003). Besides, the randomly dispersed steel fiber improve some properties of concrete like ductility, lower drying shrinkage, flexural toughness, f_f and f_{st} (Zhang *et al*. 2014). Moreover, the efficiency of mini fiber fairly bounds up with their degree of scattering in the concrete mixture (Giner *et al*. 2011). They considerably contribute to decreasing and restraining the crack breadths. Hence, it can be beneficial to utilize steel fiber as a complement to traditional reinforcement for crack prevention (Berrocal *et al*. 2013). Because of this, steel fiber reinforcement may be utilized to meaningfully decrease the permeability of concrete, thus enhance the durability, and service life (Abbas 2013).

Several experimental studies have been performed by the utilization of steel fiber in concrete containing various mineral admixtures. Some studies performed on the effect of steel fiber on mechanical properties of concrete made with mineral admixtures like MK, GP, silica fume, ground blast furnace slag and fly ash were made by Güneyisi *et al*. (2014), Shaaban and Gesund (1993), Rashiddadash *et al*. (2014), Atiş and Karahan (2009), Holschemacher *et al*. (2010), Gesoğlu *et al*. (2013), El-Dieb (2009), Eren and

*Corresponding author, Ph.D.,
E-mail: msdemir@nigde.edu.tr; msdemir@ohu.edu.tr

ISSN: 1229-9367 (Print), 1598-6233 (Online)

Çelik (1997), Nili and Afroughsabet (2012), Köksal *et al*. (2008), Giner *et al*. (2012), Kaikea *et al*. (2014), Bernal *et al*. (2010) and Hwang *et al*. (2015). It has been proved in the studies that the use of steel fiber can meaningfully enhance the mechanical behaviors of concrete. The effect of steel fiber and MK combinations on the f_f, f_{st}, f_c and bonding strength of concrete were investigated by Güneyisi *et al*. (2014). They used two types of steel fiber and 10% MK in the concrete mixes at water-binder ratios of 0.35 and 0.50. Their experimental results show that using the combinations of MK and different types of steel fiber in concrete importantly influenced the strength properties of concrete compared to control concrete. Particularly, they stated that the type of the steel fiber had the biggest impact for bonding strength and f_f values of concrete. Shaaban and Gesund (1993) researched the influence of steel fiber on the f_c and f_{st} values of concrete. Rashiddadash *et al*. (2014) researched the effect of hybrid fibers on the f_f and f_c values of concretes produce with different amounts pumice and MK. They used pumice and MK to replace cement with 10% and 15% ratios in the reinforced concretes made with 0.75% steel fiber and 0.25% polypropylene fiber dosages by volume. They reported that the mechanical properties of hybrid fiber reinforced concretes made with higher steel fiber dosage were comparatively better than less steel fiber dosage. In addition, they reported that the f_c values of concretes made with pumice were lower than that of control concretes at all times, while the f_c values of concretes made with MK were higher than that of control concretes at all times. Atiş and Karahan (2009) researched the influence of steel fiber on the f_c and f_f values of concrete made with fly ash. They used fly ash to replace cement with 0%, 15% and 30% ratios in the reinforced concretes with 0%, 0.25%, 0.5%, 1.0% and 1.5% steel fiber in volume. They stated that a small increase with increasing fiber content was observed on the f_c values of concretes made with fly ash. They also reported that the f_f values of reinforced concretes made with higher steel fiber dosage were comparatively higher than less steel fiber dosage. Besides, they reported that there was any positive effect of the addition of steel fiber on the modulus of elasticity. The influence of steel fiber types on the f_{st} and f_c values of concrete made with fly ash was investigated by Holschemacher *et al*. (2010). They stated that the strength values increase as the amount of fiber increases. The influence of two steel fiber types and silica fume combinations on the f_c, f_f and bonding strength values of concretes made with cold bonded fly ash aggregates were investigated by Gesoğlu *et al*. (2013). They reported that the inclusion of steel fiber exhibited notable improvement in the f_c, f_f and bonding strength values capacities of concretes. They also reported that the long fiber reinforced concretes provided higher strength development than short fiber reinforced concretes. El-Dieb (2009) investigated the effect of steel fiber on the f_c and f_{st} values of ultra-high strength self-compacting concrete. The author stated that the f_c and f_{st} values are enhanced by the addition of steel fiber in the concrete mixture. The effect of steel fiber on the f_c and f_{st} values of concrete containing silica fume was investigated by Eren and Çelik (1997). They stated that the addition of steel fiber provided notable improvement on the f_c and f_{st} values of concrete containing silica fume when compared to plain ones. Nili and Afroughsabet (2012) investigated the influence of added steel fiber on the early- and long-term f_c of concrete containing silica fume. They stated that the addition of the higher fiber led to higher f_c. Köksal *et al*. (2008) investigated the combined effect of steel fiber and silica fume on the f_c, f_f, f_{st} and elastic modulus values of high strength concretes. They stated that the use of steel fiber in combination with silica fume exhibited better performance compared to the concretes containing only steel fiber or only silica fume. The influence of added steel fiber and carbon fiber on the f_c, f_f and dynamic properties of concrete made with silica fume was investigated by Giner *et al*. (2012). In contrast to other studies, they stated that both carbon fiber and steel fiber additions led to slight reduces of the f_c value of concrete. Kaikea *et al*. (2014) researched the effect of silica fume and blast furnace slag on the f_c and f_f values of steel fiber reinforced high performance concrete. They used the steel fiber at proportions of 0%, 0.5% and 1% by volume of concrete. They stated that the addition of steel fiber had a significant influence on the f_c and f_f values of high performance concrete. Bernal *et al*. (2010) investigated the f_c, f_f and f_{st} values of steel fiber reinforced an alkali-activated slag concrete at early ages. They reported the addition of steel fiber exhibited a decrease in the f_c value of both cement concrete and an alkali-activated slag concrete, while the f_{st} value increase in both concrete produced with cement and concrete produced with alkali-activated slag.

In this study, the effect of MK, GP and combination of MK and GP on the mechanical properties of steel fiber reinforced concrete (SFRC) obtained by replacing cement with MK, GP and combination of MK and GP at proportions of 5%, 10%, 15% and 20% by weight were investigated. Totally, 16 SFRC mixtures were produced with a low water-binder ratio of 0.2. A type of steel fiber with length and aspect ratio (length/diameter) of 33 mm and 44 was utilized in these mixtures. The U_{pv}, f_c, f_f and f_{st} tests on the produced concrete specimens were executed. Moreover, the correlations between the f_c and other properties of SFRHSCs were executed by way of the experimental results. Besides, two alternative GEP-based models are proposed for predicting the f_c of SFRHSC made with binary and ternary blends of MK and GP. First model is proposed for predicting the f_c from the age of specimen and amounts of concrete mixtures of SFRHSC made with made with binary and ternary blends of MK and GP, which is called as GEP-I, and second model is proposed for predicting the f_c from unit weight (UW) and U_{pv} of SFRHSC made with binary and ternary blends of MK and GP, which is called as GEP-II.

2. Experimental study

2.1 Materials

ASTM type I Portland cement, manufactured in Turkey as CEM I 42.5 R type Portland cement that correspond to TS EN 197-1 (2004), was employed in the concrete mixtures. The Portland cement was supplied from the

cement plant of ÇİMSA Niğde in Turkey. Blaine fineness and specific gravity values of the utilized cement were 332 m^2/kg and 3.04, respectively. MK called as Metamax was utilized for replacement with cement. The used MK was provided from BASF-The Chemical Company. MK meets all of the specifications of ASTM C618-12a (2012) Class N pozzolans. The tamped bulk density and specific gravity values of MK were 480 kg/m^3 and 2.50, respectively. The GP used in this study was provided from Nevşehir Mikromin Company in Turkey. The density and specific gravity values of GP were 290 kg/m^3 and 2.46, respectively. The compositions of cement, MK and GP are presented in Table 1.

The fine aggregates were a mixture of natural basalt sand-I (NS-I) and natural quartz sand-II (NS-II) with maximum size of 0-1 mm and 0-5 mm, respectively. The coarse aggregates were a mixture of crushed limestone-I (CL-I) and crushed limestone-II (CL-II) with particle size of 5-12 mm and 12-22 mm, respectively. The aggregates used in the concrete mixtures were supplied from local resources. The sieve analysis and physical properties of aggregates are given in Table 2. The steel fiber called as MasterFiber FS3N containing low carbon was added to concrete mixtures. This fiber was provided from BASF-The Chemical Company. The used steel fiber meets all of the specifications of ASTM A820/A820M (2011). The ends of this fiber were mechanically warped in order to supply maximum adhesion between the cement paste and steel fiber. The properties of the steel fiber are also given in Table 3. The chemical admixture, called as Glenium 51 and used in concrete mixtures, was provided from BASF-The Chemical Company. This innovative admixture, based on modified polycarboxylic ether polymers founded high range water decreasing admixture with specific gravity of 1.095, was used to obtain slump value as 8±2 cm in concrete mixtures. The admixture ratio used in the concrete mixtures was modified at the time of mixing to obtain the designated slump.

Table 1 Chemical composition of binders

Binder	Oxide (%)								
	SiO_2	Al_2O_3	Fe_2O_3	CaO	MgO	SO_3	K_2O	Na_2O	LOI*
Cement	22.35	4.50	2.40	63.20	2.50	2.80	0.60	0.70	0.95
MK	67.90	14.20	2.15	2.50	0.84	0.70	3.44	5.91	2.36
GP	54.00	45.10	0.42	0.02	0.03	0.01	0.20	0.22	-

* LOI: Loss on ignition (%)

Table 2 Sieve analysis and physical properties of aggregates

Sieve size, (mm)		Passing (%)				
		Fine aggregate		Coarse aggregate		Total used aggregate
		NS-I* 0-1 mm	NS-II 0-5 mm	CL-I 5-12 mm	CL-II 12-22 mm	0-22 mm
Sieve analysis	31.5	100.00	100.00	100.00	100.00	100.00
	22.4	100.00	100.00	100.00	100.00	100.00
	16	100.00	100.00	100.00	71.80	90.13
	11.2	100.00	100.00	98.92	20.35	71.85
	8	100.00	100.00	78.36	0.74	59.85
	5.6	99.80	99.60	42.20	0.00	50.41
	4	99.70	93.90	12.04	0.00	41.15
	2	99.50	73.10	2.02	0.00	32.39
	1	99.20	38.62	0.50	0.00	21.63
	0.5	95.20	21.75	0.06	0.00	16.06
	0.25	51.90	9.50	0.00	0.00	8.04
	0.15	18.30	8.73	0.00	0.00	4.5
	0.63	9.20	3.62	0.00	0.00	2
Amounts of mixture	%	10	30	25	35	
Physical properties	Specific gravity	2.53	2.48	2.71	2.73	
	Ab., %	0.65	0.80	0.40	0.35	

* NS: Natural sand; CL: Crushed limestone; Ab.: Absorption

Table 3 Properties of steel fiber

Length (mm)	Diameter (mm)	Aspect ratio (%)	Tensile strength MPa	QF (units per kg)
35	0.75	44	1100	8738

* QF: Quantity of fiber

2.2 Mixture proportions

Three series of concrete mixtures, which are apart from the control mixture, with water-binder ratio of 0.20 were designed to manufacture SFRCs. The ratios of concrete mixtures are given in Table 4. These concrete mixtures were planned as possessing total binder and steel fiber ingredient of 500 kg/m^3 and 50 kg/m^3, respectively. The control mixture consisted of only Portland cement as the binder while the remainder mixtures included the 5%, 10%, 15% and 20% MK (5 MK, 10 MK, 15 MK and 20 MK) in the first series as binary binders, the 5%, 10%, 15% and 20% GP (5 GP, 10 GP, 15 GP and 20 GP) in the second series as binary binders and 2.5% MK + 2.5% GP, 5% MK + 5% GP, 5% MK + 10% GP, 5% MK + 15% GP, 10% MK + 5% GP, 10% MK + 10% GP and 15% MK + 5% GP (2.5 MK + 2.5 GP, 5 MK + 5 GP, 5 MK + 10 GP, 5 MK + 15 GP, 10 MK + 5 GP, 10 MK + 10 GP and 15 MK + 5 GP) in the third series as ternary binders.

2.3 Test specimens

After the complete steel fiber reinforced concretes (SFRCs) were mixed according to ASTM C192/ C192M-14 (2000) in a pan type mixer, the necessary specimens were molded and compressed by a vibrating table. The produced fresh concrete specimens were covered with wet towel and hold in laboratory at 22±2°C for a day. Afterwards, these specimens removed from the mold were stored in a water-curing tank up to the time of testing. The 10×10×10 cm

Table 4 Mixture proportions of steel fiber reinforced concretes (kg/m^3)

Series	Mixture code	Cement kg/m³	MK kg/m³	GP kg/m³	Water kg/m³	NS-I kg/m³	NS-II kg/m³	CL-I kg/m³	CL-II kg/m³	Fiber kg/m³	SP kg/m³
	C*	500	0	0.00	100	253.33	533.94	486.22	685.73	50	15.00
First	5 MK	475	25	0.00	100	252.67	532.54	484.94	683.93	50	15.83
	10 MK	450	50	0.00	100	252.01	531.14	483.66	682.13	50	16.67
	15 MK	425	75	0.00	100	251.34	529.74	482.39	680.33	50	17.50
	20 MK	400	100	0.00	100	250.68	528.34	481.11	678.53	50	18.33
Second	5 GP	475	0.00	25	100	252.36	531.89	484.35	683.10	50	15.00
	10 GP	450	0.00	50	100	251.39	529.84	482.49	680.47	50	18.33
	15 GP	425	0.00	75	100	250.42	527.80	480.62	677.84	50	20.00
	20 GP	400	0.00	100	100	249.45	525.75	478.76	675.21	50	21.67
Third	2.5 MK + 2.5 GP	475	12.5	12.5	100	252.52	532.22	484.65	683.51	50	15.00
	5 MK + 5GP	450	25	25	100	251.70	530.49	483.08	681.30	50	15.83
	5 MK + 10 GP	425	25	50	100	250.73	528.44	481.21	678.67	50	20.00
	5 MK + 15 GP	400	25	75	100	249.75	526.40	479.35	676.04	50	21.67
	10 MK +5GP	425	50	25	100	251.03	529.09	481.80	679.50	50	18.33
	10MK+10GP	400	50	50	100	250.06	527.04	479.93	676.87	50	20.83
	15MK+5GP	400	75	25	100	250.37	527.69	480.52	677.70	50	19.17

* C: Control concrete; MK: Metakaolin; GP: Ground pumice; SP: Superplasticizer; CL: Crushed limestone

cube specimens were used to obtain the U_{pv} and f_c values at the ages of 7, 28 and 56 days. Besides, the 15×15×15 cm cube specimens were used to determine the f_c at the age of 56 days. Moreover, the 15×15×15 cm cube and 10×10×40 cm prism specimens were used to obtain the f_{st} and f_f values at the age of 56 days, respectively.

2.4 Test methods

The U_{pv} determined on SFRC specimens at the ages of 7, 28 and 56 days in accordance with the following equation

$$U_{pv} = \frac{S}{t} \times 10 \quad (1)$$

Where U_{pv} is the ultrasonic pulse velocity (km/s), S is the length of the straight wave path through the sample (cm) (i.e., 10 cm in this work), and t is the pass time of the ultrasonic pulse through S (μs) measured by ultrasonic pulse velocity tester machine. The f_c values of SFRC specimens were determined by using the test methods according to TS EN 12390-3 (2010) and ASTM C39/C39M-14a (2012) at the ages of 7, 28 and 56 days. The f_f values of SFRC specimens were determined on the prismatic specimens by three points loading test according to TS EN 12390-5 (2010) at the age of 56 days. The f_{st} values of SFRC specimens were carried out by applying linear load on the top and bottom of the cube specimens according to TS EN 12390-6 (2010) at the age of 56 days.

3. Experimental study results and discussion

3.1 Ultrasonic pulse velocity

Ultrasonic pulse velocity (U_{pv}) in a material relates to the porousness, compactness and elastic properties of the material. The influences of MK, GP and combination of MK and GP on the U_{pv} values of SFRC specimens were evaluated by ultrasonic measurements executed in this study. Fig. 1 shows the U_{pv} values obtained from the ultrasonic measurements of all the SFRC specimens at the ages of 7, 28 and 56 days. Each U_{pv} result represents the average of three measurements. As seen in Fig. 1, the U_{pv} values of SFRC specimens increase together with the increasing curing days. In the first series, it can be observed that the SFRCs made with 5%, 10% and 15% MK reveal higher U_{pv} values than control concrete at the ages of 7, 28 and 56 days, while the U_{pv} values tends to reduce for 20%. In this series, it is observed that the best mixture for highest U_{pv} value is the concrete mixture with 10% MK. In this series, the increases of U_{pv} values were about 1.5%, 1.5% and 1% at the ages of 7, 28 and 56 days, respectively. Effect of MK content on the U_{pv} value of specimens cured in water and in air was investigated by Khatib (2008). His results revealed that the best replacement ratio was 12.5% for water cured and 7.5% for air cured. The author observed that there was little difference in the U_{pv} values between the two curing methods. In the second series, it can be shown from Fig. 1 that the U_{pv} values reduce with increasing GP substitution for cement at the ages of 7, 28 and 56 days except for concrete containing 5% GP. In the third series, all SFRCs made with ternary blends have higher the U_{pv} comparing to control concrete at all curing days except for concrete containing 5% MK + 15% GP. In this series, maximum increase in the U_{pv} values occurred at 5% MK + 5% GP replacement and it was about 1% at all day curing times. In general, the U_{pv} values of SFRCs made with binary blends of GP decrease, while the U_{pv} values of SFRCs made with binary blends of MK and combination of

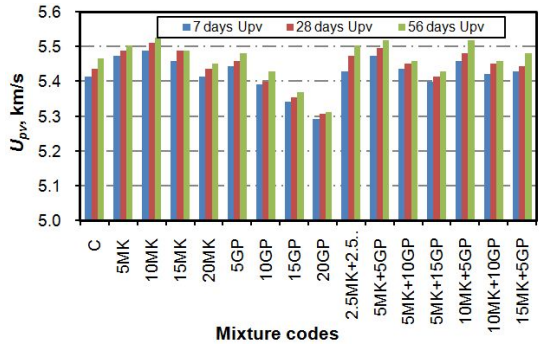

Fig. 1 The U_{pv} values of SFRHSC made with binary and ternary blends of MK and GP

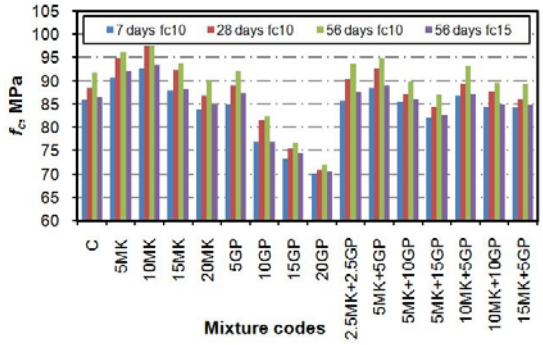

Fig. 2 The f_c values of SFRHSC made with binary and ternary blends of MK and GP

MK and GP increase. This is why the GP has more porosity compared to that of MK.

3.2 Compressive strength

The 10×10×10 cm cube compressive strength (f_{c10}) values evolvement of SFRCs made with binary and ternary blends of MK and GP at the ages of 7, 28 and 56 days are shown in Fig. 2, where each f_{c10} value is averaged from the results of three 10×10×10 cm cube specimens. Besides, the f_{c10} and the 15×15×15 cm cube compressive strength (f_{c15}) values of same concretes at the age of 56 days are given in Table 5. The f_{c10} value of the control mixture at the age of 7 days was obtained to be 85.93 MPa that enlarged to 88.39 and 91.72 MPa with an increase of about 3% and 7% at the ages of 28 and 56 days, respectively. It can be obviously shown from Fig. 2 that the f_{c10} values of the steel fiber reinforced control concrete perform lower than those of SFRCs made with all binary blends of MK, binary blends of 5% GP and ternary blends of 2.5% MK + 2.5% GP, 5% MK + 5% GP and 10% MK + 5% GP. In the binary blends of MK and GP series, it is observed that the best combinations for enhancing f_{c10} value are the SFRC mixtures made with binary blends of 10% MK and binary blends of 5% GP at the ages of 7, 28 and 56 days. The increases in the f_{c10} according to control concrete were observed as about 8%, 10% and 6% at the ages of 7, 28 and 56 days in the binary blends of 10% MK. In the binary blends of GP series, it was observed that the f_{c10} values reduced with increasing GP replacement ratio. However, in this series, for 5% GP replacement ratio, the f_{c10} value was nearly similar to the f_{c10} value of control concrete. In the ternary blends of MK+GP series, it is determined that the best combination for improving f_{c10} value is the SFRC mixture made with ternary blends of 5% MK + 5% GP at the ages of 7, 28 and 56 days. The f_{c10} values of the ternary blends of 5% MK + 5% GP were observed as 88.44, 92.66 and 94.97 MPa at the ages of 7, 28 and 56 days. The f_{c15} values of same concretes at the age of 56 days are nearly similar to the f_{c10} values of same concretes at the age of 56 days.

Table 5 Normalized f_c, f_{st} and f_{fs} values of SFRHSC

Mixtures	f_{c10i}/f_{c10}*			f_{c15i}/f_{c15}	f_{sti}/f_{st}	f_{fsi}/f_{fsi}
	7 days	28 days	56 days	56 days	56 days	56 days
C	1.00	1.00	1.00	1.00	1.00	1.00
5 MK	1.06	1.07	1.05	1.07	1.03	1.08
10 MK	1.08	1.10	1.06	1.08	1.04	1.11
15 MK	1.02	1.04	1.02	1.02	1.02	1.04
20 MK	0.98	0.98	0.98	0.98	0.99	0.99
5 GP	0.99	1.01	1.00	1.01	1.01	1.04
10 GP	0.89	0.92	0.90	0.89	0.98	0.93
15 GP	0.85	0.85	0.84	0.86	0.96	0.89
20 GP	0.82	0.80	0.79	0.82	0.94	0.83
2.5 MK + 2.5 GP	1.00	1.02	1.02	1.01	1.01	1.05
5 MK + 5 GP	1.03	1.05	1.04	1.03	1.02	1.06
5 MK + 10 GP	0.99	0.99	0.98	1.00	1.00	0.99
5 MK + 15 GP	0.95	0.96	0.95	0.96	0.98	0.96
10 MK + 5 GP	1.01	1.01	1.02	1.01	1.01	1.03
10 MK + 10 GP	0.98	0.99	0.98	0.98	0.99	0.97
15 MK + 5 GP	0.98	0.97	0.97	0.98	0.99	0.98

* $f_{c10\text{ or }c15}$: C; $f_{c10i\text{ or }c15i}$: C … 15 MK + 5 GP;
f_{st}: C; f_{sti}: C … 15 MK + 5 GP; f_f: C; f_{fi}: C … 15 MK + 5 GP

Similar experimental results with regard to the improvement of f_c values of SFRCs containing MK were observed in the previous studies (Güneyisi *et al*. 2014, Rashiddadash *et al*. 2014). In the study of Güneyisi *et al*. (2014), the f_c values of SFRCs made with 10% MK replacement ratio obtained comparatively higher than that of control concretes at water-binder ratios of 0.35 and 0.50. Similarly, Rashiddadash *et al*. (2014) observed that MK was very effective on the f_c value evolvement and the utilize of MK at 10% and 15% replacement ratio enhanced the f_c values of SFRCs at the ages of 7, 28, 90 and 180 days according to the utilize of GP at 10% and 15%. As indicated in these experimental studies, the binary blends of MK increase f_c value not only at the early-days but also at later-days. The MK content in the cement matrix enhances the bond between the aggregate particles and the cement paste in addition to improving the density of cement paste, which in turn meaningfully increases the f_c value of concrete

(Rashiddadash *et al*. 2014).

3.3 Flexural and splitting tensile strengths

The flexural strength (f_f) and splitting tensile strength (f_{st}) values of SFRCs made with binary and ternary blends of MK and GP at the age of 56 days are given in Fig. 3 and Table 5. Each value in this figure represents the average f_f and f_{st} values of three 10×10×40 cm prism and 15×15×15 cm cube specimens, respectively. As seen in Fig. 3 and Table 5, the f_f and f_{st} values of the steel fiber reinforced control concrete perform lower than all SFRCs made with binary blends of MK except for 20% MK mixture at the age of 56 days. On the other hand, as seen in Fig. 3 and Table 5, the f_f and f_{st} values of the control concrete perform better than all SFRCs made with binary blends of GP except for 5% GP mixture at the age of 56 days. The high increases in the f_f and f_{st} values according to control concrete for the binary blends of MK determined as approximately 11% and 4% for 10% MK contents, while the high decreases in the f_f and f_{st} values according to control concrete for the binary blends of GP determined as approximately 17% and 6% for 20% GP contents, respectively. It can be obviously shown from Fig. 3 and Table 5 that the f_f and f_{st} values of SFRCs made with ternary blends MK and GP except for 5% MK + 15% GP, 10% MK + 10% GP and 15% MK + 5% GP are higher than that of control concrete. The maximum f_f and f_{st} values were observed as 10.34 and 5.64 MPa for SFRC made with ternary blends of 5% MK + 5% GP. In the all series, the maximum f_f and f_{st} values were observed as 10.84 and 5.77 MPa for SFRC made with binary blends of 10% MK, respectively. In fact, the ternary blends of MK + GP generally reduced the difference in the f_f and f_{st} values compared to the concretes with binary blends of GP.

In the study of Güneyisi *et al*. (2014), the effect of MK on the f_f and f_{st} values of SFRCs were investigated. They indicated that the f_f and f_{st} values of concrete made with 10% MK replacement ratio obtained comparatively higher than that of control concrete at water-binder ratios of 0.35 and 0.50. They also revealed that the steel fiber addition provided the increase in the f_f and f_{st} capacity of control concrete. Rashiddadash *et al*. (2014) also used MK and GP as a cementitious material to increase f_f and f_{st} values of hybrid fiber reinforced concrete. They reported that the f_f and f_{st} values of hybrid fiber reinforced concrete containing 10% and 15% MK were higher than that of control concrete, while the f_f and f_{st} values of hybrid fiber reinforced concrete containing 10% and 15% GP were lower than that of control concrete.

4. Correlations between mechanical properties

In this study, the correlations between the U_{pv}, f_{c10}, f_{st} and f_{fs} values of SFRHSCs made with binary and ternary blends of MK and GP were appraised by the linear regression models.

4.1 Correlation between U_{pv} and f_c

In the recent years, the correlation between the U_{pv} and f_{c10} values has been carried out by many researchers (Demirboğa *et al*. 2004, Hamid *et al*. 2010, Shariq *et al*. 2013, Nik and Omran 2013). The U_{pv} value of concrete is influenced by alteration in the cement paste that is affected by water-binder ratio and moisture situation of concrete. The U_{pv} value is also affected by the compactness and density of concrete. Despite these restrictions, the U_{pv} can be utilized to evaluate the f_{c10} of concrete. Besides, these restrictions influence the f_{c10} of concrete because of the supplement of mineral admixtures in the concrete mixtures (Shariq *et al*. 2013). Hence, the correlation between U_{pv} and f_{c10} values of concrete has been carried out. Fig. 4 exhibits the correlation between the U_{pv} and f_{c10} values of SFRHSCs made with binary and ternary blends of MK and GP at the ages of 7, 28 and 56 days. It can be obviously shown from this figure that there are strong correlations between the U_{pv} and f_{c10} values of SFRHSCs made with binary and ternary blends of both MK and GP. These strong correlations between the U_{pv} and f_{c10} values are obviously verified by the trend line and R-square (R^2) values given in Fig. 4. Besides, the f_{c10} value can be calculated from U_{pv} value by the Eq. (2) given in this figure.

$$f_{c10} = 0.032e^{1.45U_{pv}} \quad (2)$$

4.2 Correlations between strength properties

The correlations of the f_f-f_c and f_{st}-f_c values were carried out by many researchers (Rashid *et al*. 2004, Xu and Shi 2009, Mo *et al*. 2014). Besides, the equations were

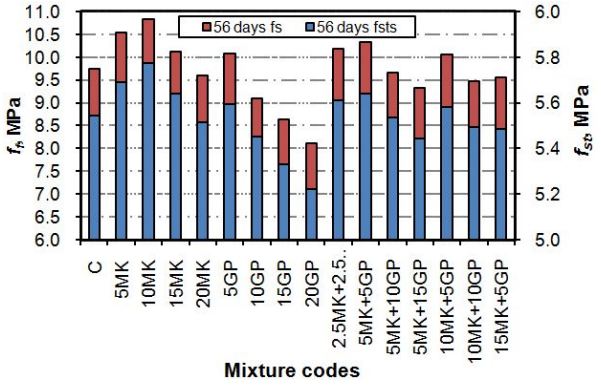

Fig. 3 The f_{st} and f_{fs} values of SFRHSC made with binary and ternary blends of MK and GP

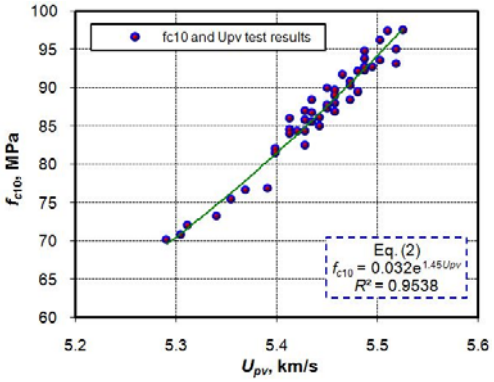

Fig. 4 Correlation between the f_{c10} and U_{pv} values

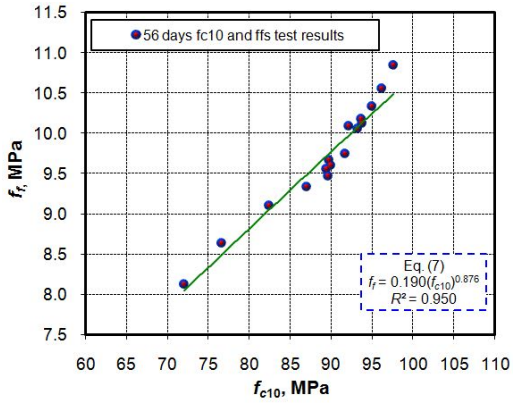

(a) Correlation between the f_f and f_{c10}

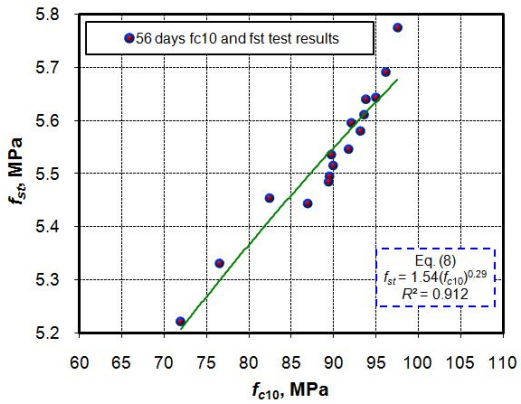

(b) Correlation between the f_{st} and f_{c10}

Fig. 5 Correlations between strength properties

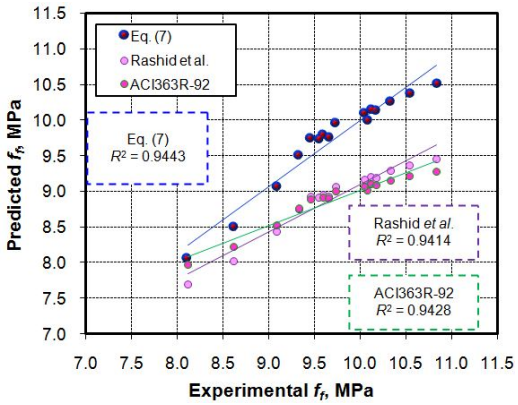

(a) Comparison of the predicted f_f and experimental f_f

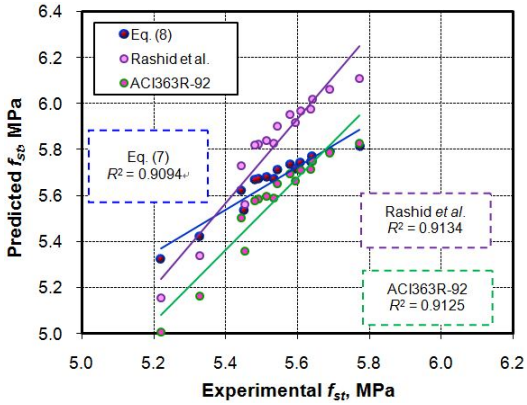

(b) Comparison of the predicted f_{st} and experimental f_{st}

Fig. 6 Comparison of the predicted f_f or f_{st} and experimental f_f or f_{st}

proposed by national building codes such as ACI363R-92 (1992) (Eqs. (3)-(4)) and ACI318R-95 (1995). Rashid *et al.* (2004) compiled a significant volume experimental data on the f_c, f_f and f_{st} values of concrete. They suggested that there were correlations of the f_f-f_c and f_{st}-f_c values of concrete by using these data according to inverse S-curve (Eqs. (5)-(6)). Xu and Shi (2009) proposed power correlations of the f_f-f_c and f_{st}-f_c values for SFRC with non-linear regression analyses. Mo *et al.* (2014) proposed the non-linear regression analyses of the f_f-f_c and f_{st}-f_c values of steel fiber reinforced oil palm shell concrete. In the present study, the correlations of the f_f-f_{c10} and f_{st}-f_{c10} values of SFRHSCs made with binary and ternary blends of MK and GP at the age of 56 days are illustrated in Fig. 5(a)-(b), respectively. The equations obtained from these correlations are compatible with the equations proposed by the researchers. As it is clear, the f_f and f_{st} values also increase by increasing f_{c10} value and the correlations between them are nonlinear. As it can be shown, a curve slope of SFRHSC made with binary blends of GP is more than that of binary blends of MK and ternary blends of MK and GP. The correlations of the f_f-f_{c10} and f_{st}-f_{c10} values of SFRHSCs made with binary and ternary blends of MK and GP at the age of 56 days can be determined by the proposed new Eqs. (7)-(8) on Fig. 5(a)-(b), respectively. Besides, the R^2 values of these proposed equations are higher than 0.91. Thus, these R^2 values indicate strong correlations between these strength properties. Moreover, Fig. 6(a)-(b) show the f_f and f_{st} values predicted by ACI318R-95 (1995), Rashid *et al.* (2004) and proposed new Eqs. (7)-(8) versus the experimental f_f and f_{st} values, respectively. R^2 values given on Fig. 6(a)-(b) demonstrate that the proposed new equations (Eqs. (7)-(8)) are suitable for calculating f_f and f_{st} values from f_{c10} values of SFRHSCs. All equations are given below.

ACI363R-92 (1992)

$$f_f = 0.94(f_{c10})^{0.5} \quad (3)$$

$$f_{st} = 0.59(f_{c10})^{0.5} \quad (4)$$

Rashid *et al.* (2004)

$$f_f = 0.42(f_c)^{0.68} \quad (5)$$

$$f_{st} = 0.47(f_c)^{0.56} \quad (6)$$

New equations

$$f_f = 0.190(f_{c10})^{0.876} \quad (7)$$

$$f_{st} = 1.54(f_{c10})^{0.29} \quad (8)$$

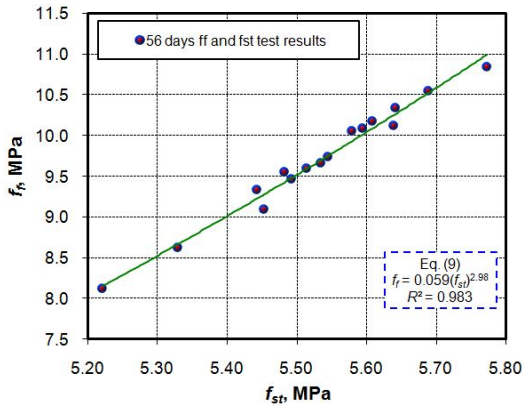

Fig. 7 Correlation between the f_f and f_{st} values

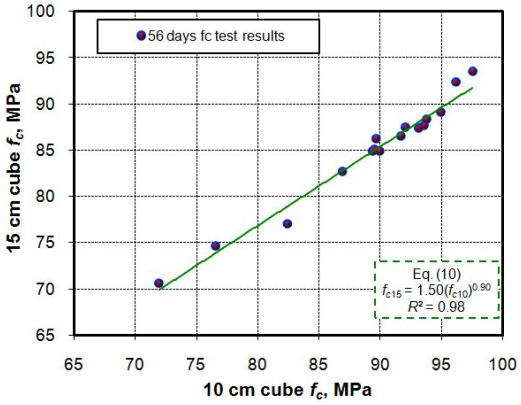

Fig. 8 Correlation between the f_{c15} and f_{c10} values

The regression analysis is performed on the experimental results of the f_f and f_{st} values of SFRHSCs as shown in Fig. 7. The empirical equation obtained from this analysis is given on Fig. 7 and by Eq. (9). Because of the corresponding R^2 values of this proposed equation is higher than 0.96, the strong correlation between the f_f and f_{st} values is seen.

$$f_f = 0.059(f_{st})^{2.98} \quad (9)$$

4.3 Size effect

Many researches were investigated the influence of specimen size on the f_c values of concretes. Some of the studies in this area were made by Yazıcı and Sezer (2007), Sim *et al*. (2013), Yi *et al*. (2006) and Nikbin *et al*. (2014). These authors used the various specimen geometries to research the size effect on the f_c of concrete. The influence of cylindrical specimen size on the f_c value of concrete was investigated by Yazıcı and Sezer (2007). They stated that the linear and nonlinear regression analyses were used for the characterization of the correlation between the f_c values of 10×20 cm and 15×30 cm cylinder specimens. They also stated that the linear and nonlinear regression analyses made between two f_c demonstrated better performance. Yi *et al*. (2006) researched the effect of cylinder, cube, and prism specimens on the f_c value of concrete by the curve-fitted using least square method. They reported that the size effect for cube and prism specimens on the f_c value of concrete become stronger than cylinders. Nikbin *et al*. (2014) researched the influences of cube specimen size and placement direction on the f_c value of self-consolidating concrete. They executed the correlations between the f_c values of various cube specimens and standard cylindrical specimens. They also expressed that the equations obtained from the curve-fitting program could be used to predict f_c values considering the effects of cube size and placement direction. In the present study, the size effect for 10×10×10 cm and 15×15×15 cm cube specimens on the f_c value of concrete are investigated. The correlation between the f_c values of 10×10×10 cm and 15×15×15 cm cube specimens at the age of 56 days is illustrated in Fig. 8. The empirical equation obtained from this correlation is also given on Fig. 8 and by Eq. (10). Because of the corresponding R^2 of this proposed equation is higher than 0.94, the strong correlation between the f_c of 10×10×10 cm and 15×15×15 cm cube specimens is seen. As shown in Fig. 8, the 10×10×10 cm cube specimens show higher f_c than 15×15×15 cm cubes. The reason of this phenomenon can be explained as small samples are exposed to lower friction-based shear forces because of the smaller contact surface between the steel platen of test machine and the sample surface in the compression test (Yazıcı and Sezer 2007, Nasser 1987). Moreover, the cohesion and gap between aggregate particles and cement paste, the number of micro-cracks and deficiencies in small samples are fewer than big samples (Sim *et al*. 2013, Yi *et al*. 2006, Nasser 1987).

$$f_{c15} = 1.50(f_{c10})^{0.90} \quad (10)$$

4.4 Microstructure analysis

The fineness of a mineral admixture used in the mixture is a significant feature with regard to filling voids within the concrete. Because the mean particle size of mineral admixture is very small more than that of cement particle, the filler influence of mineral admixture may be as significant like its pozzolanic influence (Keleştemur and Demirel 2010). In addition, a mineral admixture is effective on the properties of concrete, because it produces extra C-S-H gel by entering into chemical reaction with cement hydration products. This reaction develops to be powerful inside the interface zone between the aggregate particles, steel fiber and the cement paste (Kaikea *et al*. 2014, Güneyisi *et al*. 2012, Jiang *et al*. 2014).

The scanning electron microscope (SEM) morphologies of control concrete, 10% MK, 5% GP and 5% MK + 5% GP are illustrated in Fig. 9. The SEM morphologies were made on the small samples taken from the randomly broken concrete specimens. Irregularly shaped particles are indicated in the SEM micrograph of SFRHSC made with binary blends of 10% MK seen in Fig. 9(b), while the micro-cracks are shown in control concrete seen in Fig. 9(a). Very porous cellular surface is revealed in the SEM micrograph of SFRHSC made with binary blends of 5% GP seen in Fig. 9(c), whereas a denser structure is shown in the SFRHSC made with ternary blends of 5% MK + 5% GP seen in Fig. 9(d).

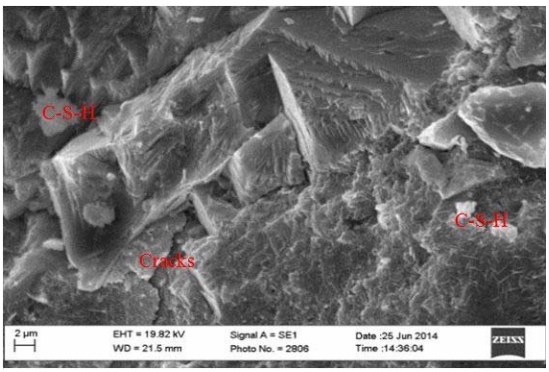

(a) Control concrete

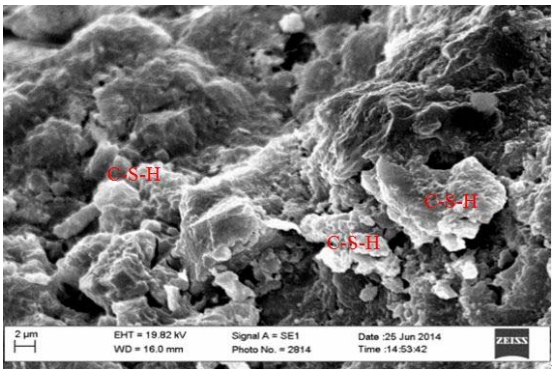

(b) %5 Metakaolin

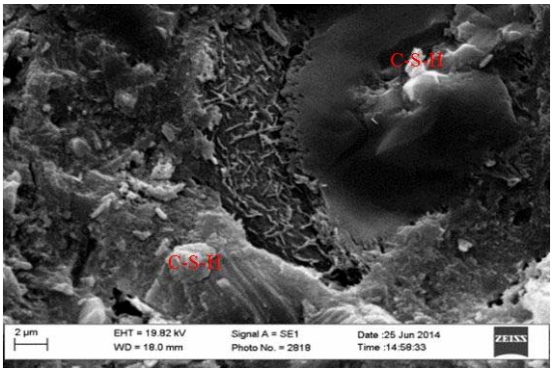

(c) %5 Ground pumice

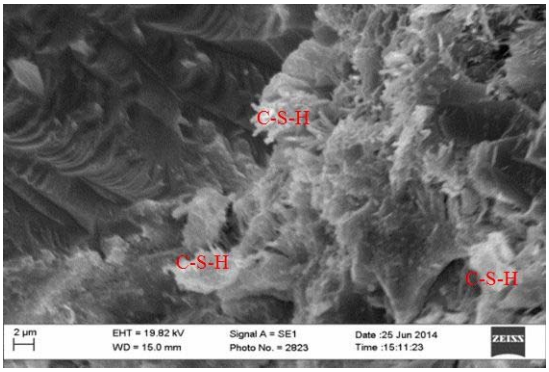

(d) %5 Ground pumice + %5 Metakaolin

Fig. 9 SEM micrographs of SFRHSC

5. Predictive study

Gene expression programming (GEP) used in this predictive study is exposed by Ferreira (2001). GEP is a natural evolvement of genetic programming and genetic algorithms. In the GEP, the individuals are encrypted as linear sequences of chromosomes which are after words declared as nonlinear existences of different sizes and forms (expression trees) (Ferreira 2001, Jedrzejowicz and Ratajczak-Ropel 2009). The chromosomes are made up of various genes, each gene coding a smaller sub-program (Nazari 2013). Any knowledge in chromosome made up of one or more genes is converted to the expression trees (ETs) applying two languages in GEP: the language of the genes and language of ETs. GEP genes composed of two pieces called as the head and tail. The head comprises symbols, which represent both terminals and functions, whereas the tail comprises only terminals. In the head, the functions may be arithmetic and trigonometric mathematical functions (+, -, *, /, sin, log) for the constituting of a mathematical equation. In the tail, the terminals are the free variables and constants of the problem (a, b, c, 1) (Ferreira 2001, Kayadelen *et al*. 2009).

The goal of evolvement of GEP-based model is to make the mathematical equation for predicting the f_c. For that goal, two models called as GEP-I and GEP-II are proposed for predicting the f_c prediction of SFRHSC made with binary and ternary blends of MK and GP. GEP-I model was developed for predicting the f_c from the age of specimen (AS), cement (C), MK, GP, water (W), NS, CL, fiber (F) and SP of SFRHSC. GEP-II model was developed for predicting the f_c from UW and U_{pv} values of SFRHSC. To build these models, among 80 experimental data presented with 16 different concrete mixtures, about 70% of the whole data (53) was separated without prior planning as training set and the remaining of the whole data (27) was used as testing set.

Firstly, in these models, single gene and two lengths of heads were employed. The number of genes, heads and the number of chromosomes were increased according to the evaluation of the performance of these models. The number of genes 5 and 2, the length of heads 6 and 6, and the number of chromosomes 20 and 30 the best performance for these models were taken, respectively. The GEP parameters employed in the training and testing sets of these models are given in Table 6.

The equations obtained from the ETs for the GEP-I and GEP-II models shown in Fig. 10-11 were given by Eqs. (11)-(12), respectively. For the GEP-I model, d0, d1, d2, d3, d4, d5, d6, d7 and d8 in Fig. 10 represent the values for input layers which are AS, C, MK, GP, W, NS, CL, F and SP, respectively. For the GEP-II model, d0 and d1 in Fig. 11 represent the values for input layers, which are UW and U_{pv}, respectively. The constants used in the GEP-I and GEP-II models are given in Table 7.

The mathematical functions are 3Rt = $\sqrt[3]{\ }$, Inv = inverse, Sqrt = $\sqrt{\ }$, X2 = square and Sub3 = subtraction with 3 inputs seen in these figures. According to the above-mentioned input variables and constants, the final equations of GEP-I and GEP-II for predicting the f_c of SFRHSC made

Table 6 GEP parameters used in these models

Inputs of GEP-I	Parameter definition	GEP-I	GEP-II
	Function set	+, -, *, /, Sqrt, 3Rt, X2, Sub3, Sin, Cos	+, -, *, Inv, 3Rt
d0 = AS	Number of chromosomes	20	30
d1 = C	Head size	6	6
d2 = MK	Number of genes	5	2
d3 = GP	Linking function	Addition	
d4 = W	Mutation	0.00138	
d5 = NS	Inversion	0.00546	
d6 = CL	OTPR*	0.00227	
d7 = F	Gene recombination	0.0027	
d8 = SP	Gene transposition	0.0027	
	Random chromosomes	0.0026	
	Constants per gene	10	

* OTPR: One and two-point recombination

Table 7 Constants used in the GEP-I and GEP-II models

	GEP-I					GEP-II	
	Sub-ETs						
Constants	1	2	3	4	5	1	2
c0					-23.093		
c1		-0.530					-4.683
c2			14.854				
c3						5.444	0.378
c4				7.748			
c5					12.100		
c6	-3.087					5.685	
c7				1.533			
c8	-4.712		3.324				
c9						3.739	

with binary and ternary blends of MK and GP are given by Eqs. (13)-(14), respectively.

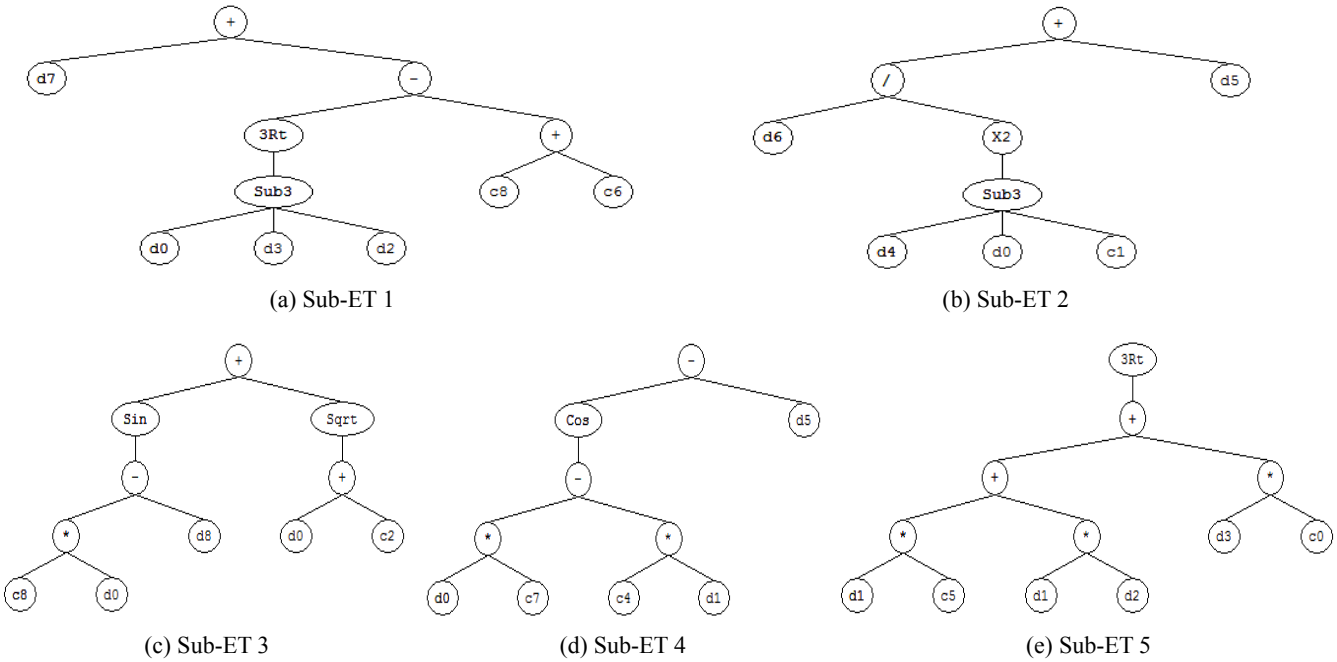

(a) Sub-ET 1 (b) Sub-ET 2

(c) Sub-ET 3 (d) Sub-ET 4 (e) Sub-ET 5

Fig. 10 Expression tree of GEP-I model used for predicting f_c

(a) Sub-ET 1 (b) Sub-ET 2

Fig. 11 Expression tree of GEP-II model used for predicting f_c

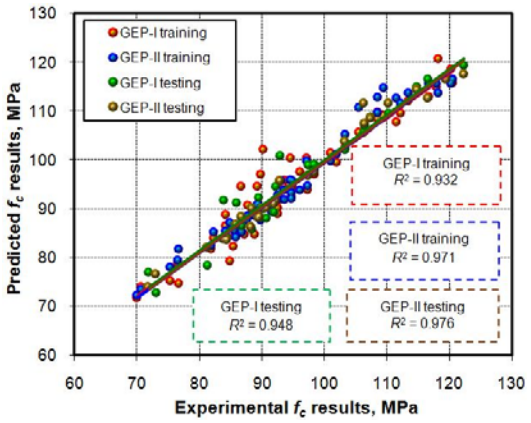

Fig. 12 Comparisons of experimental and predicted results

$$f_{c\text{-GEP-I}} = (d7 + (((d0 - d3 - d2)^{(1/3)}) - (c8 + c6))) + ((d6 / (d4 - d0 - c1)^2) + d5) + (\sin(c8 \times d0 - d8) + ((d0 + c2)^{(1/2)})) + (\cos(d0 \times c7 - c4 \times d1) - d5) + ((d1 \times c5 + d1 \times d2 + d3 \times c0)^{(1/3)}) \quad (11)$$

$$f_{c\text{-GEP-II}} = (1 / ((((c3 - d1) + (1 / c6)) \times (c6 - c9)))) + ((((d1 + c4) - c1) \times (d0)^{(1/3)}) \times d1) \quad (12)$$

$$f_{c\text{-GEP-I}} = \left(F + \sqrt[3]{AS\text{-}GP\text{-}MK} + 7.799\right) + \left(\frac{CL}{(W\text{-}AS + 0.53)^2} + NS\right) + \left(\sin(3.324AS - SP) + \sqrt{AS + 14.854}\right) + \left(\cos(1.533AS - 7.748C) - NS\right) + \left(\sqrt[3]{12.10C + C \times MK - 23.093GP}\right) \quad (13)$$

$$f_{c\text{-GEP-II}} = \frac{1}{(10.937 - 1.946U_{pv})} + (U_{pv} - 4.305) \times \sqrt[3]{UW} \times U_{pv} \quad (14)$$

6. Predictive study results and discussion

Gene expression programming (GEP) used in this predictive study is exposed by Ferreira (2001). This section mainly examines the analyses of results predicted from the GEP-I and GEP-II models and quantitative evaluations of the predictive abilities of these models. In order to disclose how exact the built models results are statistical parameters were used like the R^2, the mean absolute percentage error (MAPE) and the root mean square error (RMSE). The functions of these parameters are given in Eqs. (15)-(17), respectively.

$$R^2 = \frac{\left(n\sum_{i=1}^{n} t_i o_i - \sum_{i=1}^{n} t_i \sum_{i=1}^{n} o_i\right)^2}{\left(n\sum_{i=}^{n} t_i^2 - (\sum_{i=1}^{n} t_i)^2\right)\left(n\sum_{i=1}^{n} o_i^2 - (\sum_{i=1}^{n} o_i)^2\right)} \quad (15)$$

Table 8 Parameters used to evaluate the model results

Statistical parameters	GEP-I		GEP-II	
	Training set	Testing set	Training set	Testing set
R^2	0.932	0.948	0.971	0.976
MAPE	2.739	2.492	1.876	1.671
RMSE	3.361	3.025	2.270	2.133

$$MAPE = \frac{1}{n}\left[\frac{\sum_{i=1}^{n}|t_i - o_i|}{\sum_{i=1}^{n} t_i} \times 100\right] \quad (16)$$

$$RMSE = \sqrt{\frac{1}{n}\sum_{i=1}^{n}(t_i - o_i)^2} \quad (17)$$

Where t is the target value, o is the output value and n is total number of data.

In order to obtain the equations and to reveal the generalization ability of models developed in the GEP, the experimental results of SFRHSC made with binary and ternary blends of MK and GP is divided training and testing sets. Fig. 12 show the equations results calculated from the GEP-I and GEP-II models versus the experimental results of SFRHSC made with binary and ternary blends of MK and GP for training and testing sets. Also, the R^2 values and the linear least square fit line are showed on the figure for the training and testing sets. As it can be obviously seen in Fig. 12, the f_c values predicted from the training and testing sets in these models are very close to the experimental results. Furthermore, Fig. 12 show how good the results of training set in the GEP-I and GEP-II models learned the nonlinear relation between the input and output variables, and the results of testing set show that these models are able to generalizing between the input and output variables with reliable good prediction.

The statistical parameter results of the GEP-I and GEP-II models calculated by the equations of R^2, MAPE and RMSE for the f_c of SFRHSC made with binary and ternary blends of MK and GP are presented in Table 8. It can be shown that the R^2 values in the GEP-I for the training and testing sets are 0.932 and 0.948, while the R^2 values in the GEP-II for these sets are 0.971 and 0.976. According to GEP-I, the best values of R^2 are observed in the sets of the GEP-II model for predicting the f_c of SFRHSC made with binary and ternary blends of MK and GP among the R^2 values. Moreover, the statistical parameter results exhibit that the equations obtained from the GEP-I and GEP-II models are able to predict the f_c of SFRHSC made with binary and ternary blends of MK and GP close to that of the experimental results.

7. Conclusions

In this study, the mechanical properties of SFRHSC made with binary and ternary blends of MK and GP are

investigated. The following conclusions can be drawn from the experimental and predicted results:

- The U_{pv}, f_c, f_f and f_{st} values of SFRHSC made with binary blends of MK except for 20% MK are higher than the steel fiber reinforced control concrete.
- The U_{pv}, f_c, f_f and f_{st} values of SFRHSC made with binary blends of GP except for 5% GP are lower than the steel fiber reinforced control concrete.
- The U_{pv}, f_c, f_f and f_{st} values of SFRHSC made with ternary blends of MK + GP except for 5% MK + 15% GP, 10% MK + 10% GP and 15% MK + 5% GP are higher than the steel fiber reinforced control concrete.
- The experimental results reveal that the optimal replacement ratios are 10% for binary blends of MK, 5% for binary blends of GP, and 5% + 5% for ternary blends of MK + GP.
- The equations obtained from relationships between the U_{pv}, f_c, f_f and f_{st} values of SFRHSC can be used to assess the strength of SFRHSC.
- The equations obtained from GEP-I and GEP-II models to predict the f_c of SFRHSC made with binary and ternary blends of MK and GP can be used. The equations are so simple that they can be employed by anybody entirely unfamiliar with GEP.

As a result, the experimental results reveal that SFRHSC can be obtained with binary and ternary blends of MK and GP. Especially, it is recommended that 10% weight of MK can be used as replacement ratio of cement in order to obtain high strength concrete with good properties. The predictive study results reveal that GEP can be used as a powerful model and it can open a new area to solve many civil engineering problems.

References

Abbas, A.-A. (2013), "The effect of steel fiber on some mechanical properties of self compacting concrete", *Am. J. Civil Eng.*, **1**(3), 102-110.

ACI Committee 318 (1995), Building code requirements for structural concrete (ACI 318-1995) and Commentary; Farmington Hills, MI, USA.

ACI Committee 363 (1992), State-of-the art report on high strength concrete (ACI 363R-92); Farmington Hills, MI, USA.

ASTM A820/A820M–11 (2011), Standard specification for steel fibers for fiber-reinforced concrete; USA.

ASTM C 192 (2000), Standard practice for making and curing concrete test specimens in the laboratory; Annual Book of ASTM Standards, Vol. 04.02.

ASTM C 39/C 39M-12 (2012), Standard test method for compressive strength of cylindrical concrete specimens; ASTM Vol.04.02, West Conshohocken, PA, USA.

ASTM C618-12a (2012), Standard specification for coal fly ash and raw or calcined natural pozzolan for use in concrete; USA.

Atiş, C.D. and Karahan, O. (2009), "Properties of steel fiber reinforced fly ash concrete", C*onstr. Build. Mater.*, **23**(1), 392-399.

Bauchkar, S.D. and Chore, H.S. (2014), "Rheological properties of self consolidating concrete with various mineral admixtures", *Struct. Eng. Mech., Int. J.*, **51**(1), 1-13.

Bernal, S., Gutierrez, R.D., Delvasto, S. and Rodriguez, E. (2010), "Performance of an alkali-activated slag concrete reinforced with steel fibers", *Constr. Build. Mater.*, **24**(2), 208-214.

Berrocal, C.G., Lundgren, K. and Löfgren, I. (2013), "Influence of steel fibres on corrosion of reinforcement in concrete in chloride environments: a review", *Fibre Concrete 2013*, Prague, Czech Republic, September.

Bui, D.D., Hu, J. and Stroeven, P. (2005), "Particle size effect on the strength of rice husk ash blended gap-graded Portland cement concrete", *Cement Concrete Comp.*, **27**(3), 357-366.

Demirboğa, R., Türkmen, İ. and Karakoç, M.B. (2004), "Relationship between ultrasonic velocity and compressive strength for high-volume mineral-admixtured concrete", *Cement Concrete Res.*, **34**(12), 2329-2336.

El-Dieb, A.S. (2009), "Mechanical, durability and microstructural characteristics of ultra-high-strength self-compacting concrete incorporating steel fibers", *Mater. Des.*, **30**(10), 4286-4292.

Eren, Ö. and Çelik, T. (1997), "Effect of silica fume and steel fibers on some properties of high-strength concrete", *Constr. Build. Mater.*, **11**(1-8), 373-382.

Ferreira, C. (2001), "Gene expression programming: A new adaptive algorithm for solving problems", *Complex Syst.*, **13**(2), 87-129.

Gesoğlu, M., Güneyisi, E., Alzeebaree, R. and Mermerdaş, K. (2013), "Effect of silica fume and steel fiber on the mechanical properties of the concretes produced with cold bonded fly ash aggregates", *Constr. Build. Mater.*, **40**, 982-990.

Giaccio, G., Sensale de, G.R. and Zerbino, R. (2007), "Failure mechanism of normal and high-strength concrete with rice-husk ash", *Cement Concrete Comp.*, **29**(7), 566-574.

Giner, V., Ivorra, S., Baeza, F.J. and Ferrer, B. (2011), "Effect of different admixtures on dynamic structural behavior of fiber reinforced concrete elements", *Proceedings of the 8th International Conference on Structural Dynamics*, *EURODYN 2011*, Leuven, Belgium, July.

Giner, V.T., Baeza, F.J., Ivorra, S., Zornoza, E. and Galao, O. (2012), "Effect of steel and carbon fiber additions on the dynamic properties of concrete containing silica fume", *Mater. Design*, **34**, 332-339.

Güneyisi, E., Gesoğlu, M., Karaoğlu, S. and Mermerdaş, K. (2012), "Strength, permeability and shrinkage cracking of silica fume and metakaolin concretes", *Constr. Build. Mater.*, **34**, 120-130.

Güneyisi, E., Gesoğlu, M., Akoi, A.O.M. and Mermerdaş, K. (2014), "Combined effect of steel fiber and metakaolin incorporation on mechanical properties of concrete", *Compos.: Part B: Eng.*, **56**, 83-91.

Guven, A. and Gunal, M. (2008), "Genetic programming approach for prediction of local scour downstream of hydraulic structures", *J. Irrig. Drain. Eng.*, **134**(2), 241-249.

Hamid, R., Yusof, K.M. and Zain, M.F.M. (2010), "A combined ultrasound method applied to high performance concrete with silica fume", *Constr. Build. Mater.*, **24**(1), 94-98.

Holschemacher, K., Mueller, T. and Ribakov, Y. (2010), "Effect of steel fibres on mechanical properties of high-strength concrete", *Mater. Design*, **31**(5), 2604-2615.

Hwang, J.-H., Lee, D.H., Park, M.K., Choi, S.-H., Kim, K.S. and Pan, Z. (2015), "Shear performance assessment of steel fiber reinforced-prestressed concrete members", *Comput. Concrete*, **16**(6), 825-846.

Jedrzejowicz, P. and Ratajczak-Ropel, E. (2009), "Agent-based gene expression programming for solving the RCPSP/max problem", *Adapt. Nat. Comput. Algor.*, **5495**, 203-212.

Jiang, C., Fan, K., Wu, F. and Chen, D. (2014), "Experimental study on the mechanical properties and microstructure of chopped basalt fibre reinforced concrete", *Mater. Design*, **58**, 187-193.

Kaikea, A., Achoura, D., Duplan, F. and Rizzuti, L. (2014), "Effect of mineral admixtures and steel fiber volume contents on the behavior of high performance fiber reinforced concrete", *Mater. Design*, **63**, 493-499.

Kayadelen, C., Gunaydın, O., Fener, M., Demir, A. and Ozvan A. (2009), "Modeling of the angle of shearing resistance of soils using soft computing systems", *Expert Syst. Appl.*, **36**(9), 11814-11826.

Kayali, O., Haque, M.N. and Zhu, B. (2003), "Some characteristics of high strength fiber reinforced lightweight aggregate concrete", *Cement Concrete Comp.*, **25**(2), 207-213.

Keleştemur, O. and Demirel, B. (2010), "Corrosion behavior of reinforcing steel embedded in concrete produced with finely ground pumice and silica fume", *Constr. Build. Mater.*, **24**(10), 1898-1905.

Khatib, J.M. (2008), "Metakaolin concrete at a low water to binder ratio", *Constr. Build. Mater.*, **22**(8), 1691-1700.

Köksal, F., Altun, F., Yiğit, İ. and Şahin, Y. (2008), "Combined effect of silica fume and steel fiber on the mechanical properties of high strength concretes", *Constr. Build. Mater.*, **22**(8), 1874-1880.

Luccioni, B., Ruano, G., Isla, F., Zerbino, R. and Giaccio, G. (2012), "A simple approach to model SFRC", *Constr. Build. Mater.*, **37**, 111-124.

Mo, K.H., Yap, K.K.Q., Alengaram, U.J. and Jumaat, M.Z. (2014), "The effect of steel fibres on the enhancement of flexural and compressive toughness and fracture characteristics of oil palm shell concrete", *Constr. Build. Mater.*, **55**, 20-28.

Nasser, K.W. and Al-Manaseer, A.A. (1987), "It's time for a change from 6x12 to 3x6 inch cylinders", *ACI Mater. J.*, **84**(3), 213-216.

Nazari, A. (2013), "Compressive strength of geopolymers produced by ordinary Portland cement: Application of genetic programming for design", *Mater. Design*, **43**, 356-366.

Neville, A.M. (1996), *Properties of Concrete*, (4th and Final Ed.), Addison Wesley Logman, England.

Nik, A.S. and Omran, O.L. (2013), "Estimation of compressive strength of self-compacted concrete with fibers consisting nano-SiO_2 using ultrasonic pulse velocity", *Constr. Build. Mater.*, **44**, 654-662.

Nikbin, I.M., Dehestani, M., Beygi, M.H.A. and Rezvani, M. (2014), "Effects of cube size and placement direction on compressive strength of self-consolidating concrete", *Constr. Build. Mater.*, **59**, 144-150.

Nili, M. and Afroughsabet, V. (2012), "Property assessment of steel-fibre reinforced concrete made with silica fume", *Constr. Build. Mater.*, **28**(1), 664-669.

Parande, A.K., Babu, B.R., Karthik, M.A., Kumaar, K.K.D. and Palaniswamy, N. (2008), "Study on strength and corrosion performance for steel embedded in metakaolin blended concrete/mortar", *Constr. Build. Mater.*, **22**(3), 127-134.

Perumal, R. (2014), "Performance and modeling of high-performance steel fiber reinforced concrete under impact loads", *Comput. Concrete*, **13**(2), 255-270.

Poon, C.S., Kou, S.C. and Lam, L. (2006), "Compressive strength, chloride diffusivity and pore structure of high performance metakaolin and silica fume concrete", *Constr. Build. Mater.*, **20**(10), 858-865.

Rashid, M.A., Mansur, M.A. and Paramasivam, P. (2004), "Correlations between mechanical properties of high-strength concrete", *J. Mater. Civil Eng.*, **14**(3), 230-238.

Rashiddadash, P., Ramezanianpour, A.A. and Mahdikhani, M. (2014), "Experimental investigation on flexural toughness of hybrid fiber reinforced concrete (HFRC) containing metakaolin and pumice", *Constr. Build. Mater.*, **51**, 313-320.

Ruano, G., Isla, F., Pedraza, R.I., Sfer, D. and Luccioni, B. (2014), "Shear retrofitting of reinforced concrete beams with steel fiber reinforced concrete", *Constr. Build. Mater.*, **54**, 646-658.

Sarıdemir, M. (2009), "Prediction of compressive strength of concretes containing metakaolin and silica fume by artificial neural networks", *Adv. Eng. Softw.*, **40**(5), 350-355.

Shaaban, A.M. and Gesund, H. (1993), Splitting tensile strength of steel fiber reinforced concrete cylinders consolidated by rodding or vibrating. *ACI Mater. J.*, **90**(4), 366-369.

Shariq, M., Prasad, J. and Masood, A. (2013), "Studies in ultrasonic pulse velocity of concrete containing GGBFS", *Constr. Build. Mater.*, **40**, 944-950.

Sim, J.-II, Yang, K.-H., Kim, H.-Y. and Choi, B.-J. (2013), "Size and shape effects on compressive strength of lightweight concrete", *Constr. Build. Mater.*, **38**, 854-864.

TS EN 12390-3 (2010), Testing hardened concrete - part 3: compressive strength of test specimens; TSE, Turkey.

TS EN 12390-5 (2010), Testing hardened concrete - part 5: flexural strength of test specimens; TSE, Turkey.

TS EN 12390-6 (2010), Testing hardened concrete - part 6: tensile splitting strength of test specimens; TSE, Turkey.

TS EN-197-1 (2004), Cements-Part 1: Compositions and conformity criteria for common cements; Turkish Standards Institute, TSE, Turkey.

Xu, B.W. and Shi, H.S. (2009), "Correlations among mechanical properties of steel fiber reinforced concrete", *Constr. Build. Mater.*, **23**(12), 3468-3474.

Yazıcı, Ş. and Sezer, G.İ. (2007), "The effect of cylindrical specimen size on the compressive strength of concrete", *Build. Environ.*, **42**(6), 2417-2420.

Yi, S.-T., Yang, E.-I. and Choi, J.-C. (2006), "Effect of specimen sizes, specimen shapes and placement directions on compressive strength of concrete", *Nucl. Eng. Des.*, **236**(2), 115-127.

Zhang, X.X., Elazim, A.M.A., Ruiz, G. and Yu, R.C. (2014), "Fracture behaviour of steel fibre-reinforced concrete at a wide range of loading rates", *Int. J. Impact Eng.*, **71**, 89-96.

CC